International Journal of Applied Engineering Research, ISSN 0973-4562 Vol. 10 No.91 (2015)

Synthesis and Characterization of AgNPs Decorated on APTMs Functionalized on MoO_3 with ZrO_2 Nanocomposite and Its Catalytic Application of Methyl Parathion

E. Prabakaran[a], K. Pandian[b] and R. Sathiyapriya[a*]
[a]*Department of Chemistry, GKM College of Engineering & Technology, New Perungalathur, Chennai -600063, India.
[b]Department of Inorganic Chemistry, Guindy Campus, University of Madras, Chennai -600025, India.
prabachem86@gmail

Abstract- MoO_3/ZrO_2 catalyst was prepared by co-precipitation method. It was calcined at 400℃ with air atmosphere. Then, MoO_3/ZrO_2 incorporated with 3-amino propyl trimethoxy siliane (APTMS) oxide to get APTMS-MoO_3/ZrO_2. Further, Trisodium Citrate capped siver nano particle (AgNP) solution was mixed with APTMS-MoO_3/ZrO_2 to form AgNPs/APTMS-MoO_3/ZrO_2 nano composite. It was characterized by UV-Visible, FT-IR, XRD and SEM. The synthesised AgNPs/APTMS-MoO_3/ZrO_2 nanocomposite was applied for photocatalytic application of Methyl parathion (MP) pesticide.

***Keywords:*AgNPs/APTMS-MoO_3/ZrO_2, photocatalytic, Methyl parathion**

I. INTRODUCTION

Pesticides are mainly applied in agricultural to control insects, weeds, moths, pathogen and microbes, etc. Overutilization of pesticides results the problems like lack of nitrogen fixation and increased toxicity level in food. Mainly, pesticides are affecting the drinking water and creating serious health problems to human and animals. The problems are mainly due to the chemical properties of organochlorine chemicals (organo phosphorous and carbamate). These pesticides contain nitrogen, phosphorous, sulfur, chlorine and heterocyclic nitrogen atoms. Therefore, they should be changed from toxic chemical to non-toxic chemicals by mineralization method. Recent, literature report confirmed the degradation path way of pesticides such as atrazine [1], pyridaben [2], methyl parathion [3], methamidophos [4], triazophos [5] and dicofol [6].

Zirconium oxide is exhibited as attractive metal oxide among the TiO_2, ZnO, CdO, PbO and Ag_2O [7]. ZrO_2 exhibited as various physical and chemical properties such as thermal conductivity, thermal expansion, oxygen ion conductivity, toughness, resistance, cutting tools, refractory materials and finally catalytic behaviors as acid catalysts [8-10]. So that, it is applied in sensors, fuel cells, ceramics and optical device [11-14]. Research works were reported using ZrO_2 with MoO_3, WO_3 and CuO by wet chemical, sol-gel and co-precipitation method to enhance the catalytic activity, chemical and physical properties [15, 16].

MoO_3 is utilized in gas sensor and catalyst [17, 18]. But, it has poor ionic and electronic conductivity [19]. To improve the conductivity of MoO_3, it is coated along with carbon nanotubes [20], graphene [21], conducting polymer [22] and used in optical switching coatings, memory devices, chemical sensors, catalyst, photography, display materials, photochromic and electrochromic devices [23-29]. MoO_3 possesses three basic polymorphs (orthorhombic, monoclinic and hexagonal). Among them, orthorhombic MoO_3 acts as better cathodic material for Li ion battery [30]. It is containing single layered structure and this layer is made up two sub-layers. MoO_3 is also formed a two dimensional structure due to vanderwaals interaction with along [010] direction, which is useful to incorporate guest molecule intercalation in layers [31]. MoO_3 is prepared in different shape such as nanowires, nanotubes, nanobelts and nanorods [32-37] with activities like electrochemical properties [38-41].

The preparation of MoO_3/ZrO_2 catalyst was done by co-precipitation method and it is calcinized at low temperature 400°C which can be exhibited as an acid catalyst. Further, this catalyst is functionlized with 3-amino propyl trimethoxy silane (APTMS) to form APTMS-ZrO_2/MoO_3, then coated with silver nanoparticles (AgNPs) to get AgNPs/APTMS-MoO_3/ZrO_2 catalyst. This synthesized catalyst was applied to photocatalytic degradation of Methyl parathion (MP) under the visible light conditions.

II. EXPERIMENTAL SECTION

A. Materials - Silver nitrate ($AgNO_3$, 99.8%), $ZrOCl_2 \cdot 8H_2O$, $(NH_4)_6Mo_7O_{24} \cdot 4H_2O$, EtOH and NaOH were purchased from Merck. Methyl Parathion (MP) pesticide and Trisodium Citrate (TSC) were obtained from Sigma Aldrich, India. Milli-Q water with resistivity of 18.1 MΩ was used in this experiment.

B. Instrumentation - UV-Visible absorption spectra were recorded on a Shimadzu UV-visible spectrophotometer (UV-1800, Japan). The morphology of the sample was observed with Scanning Electron Microscopy (SEM) HITACHI Ltd (SU-6600). The X-ray Diffraction (XRD) pattern was taken with a Philips instrument (JSO Debye Flex 2002 Seifert) in the angular range 10^{o} to 80^{o}. Fourier Transform Infrared Spectroscopy (FT-IR) spectra were recorded using a Perkin-Elmer, USA (Model Y 40) in the range of 4000 - 400 cm^{-1}.

C. Synthesis of AgNPs. - Silver nanoparticles were prepared with 0.01 M of $AgNO_3$ was dissolved in 100 ml MQ water boiled at 100℃ for 1hrs. Boiled solution of $AgNO_3$ kept at room temperature with stirring. The drops wise solution of 0.1 M of Trisodium Citrate (TSC) was added into boiled silver nitrate solution to change yellow color solution which indicates the AgNPs.

D. Synthesis of MoO_3/ZrO_2 - Synthesis of MoO_3/ZrO_2 was done by using an equal molar of 0.01 M solution at zirconium chloride octahydrate ($ZrOCl_2{\cdot}8H_2O$) and ammonium heptamolybdate $(NH_4)_6Mo_7O_{24}{\cdot}4H_2O$, which were dissolved in 50 ml distilled water with constant stirring at room temperature for 10 minutes. 0.5 g of sodium hydroxide was dissolved in 10 ml of Milli-Q water then added drop wise to the homogenous precursor solution of MoO_3/ZrO_2 to reach pH 10. The white precipitate obtained was washed with Milli-Q water and ethanol to leave the unwanted precursor solutions. Finally, the solid material was collected and calcined at 400 °C for 4 hr.

E. Synthesis of AgNPs/APTMS-MoO_3/ZrO_2 nanocomposite - 1.0 g of MoO_3/ZrO_2 was dispersed in 20 ml of ethanolic solution of APTMS (2.0 ml) and stirred for 2hr. Then 0.5 g of APTMS-MoO_3/ZrO_2 was mixed with synthesized 10 ml of TSC capped AgNPs solution and kept in 12 hrs. Finally, AgNPs/APTMS- MoO_3/ZrO_2 nanocomposite was washed with Milli-Q water at dried at room temperature. The resulting AgNPs was characterized and used as photocatalyst for the degradation methyl parathion.

III. RESULT AND DISCUSSION

A. AgNPs/APTMS-MoO_3/ZrO_2 nanocomposite - Synthesis of AgNPs/APTMS-MoO_3/ZrO_2 nanocomposite was done by co-precipitation and wet chemical methods. In which MoO_3/ZrO_2 was prepared from $ZrOCl_2{\cdot}8H_2O$, $(NH_4)_6Mo_7O_{24}{\cdot}4H_2O$ as precursor followed by sodium hydroxide solution at pH 10 with stirring for 30 Min. The white precipitate was formed, centrifuged and dried at room temperature. This precipitate was calcined at 400 ^{0}C. Further, the calcined MoO_3/ZrO_2 was dispersed in ethanol solution of APTMS and kept for 12 hrs then dried at room temperature to get APTMS functionalized ZrO_2/MoO_3. Since, APTMS contains silane and amino groups, in which silane group coordinate with hydroxyl group of MoO_3/ZrO_2 due to hydrogen bond formation. Finally, addition of AgNPs solution was taken place with APTMS-MoO_3/ZrO_2 to get AgNPs/APTMS-MoO_3/ZrO_2 nanocomposite as shown in **Fig.1**. In which AgNPs adsorbed on the amine group of APTMS due to Vander Waals interaction with mechanism described below.

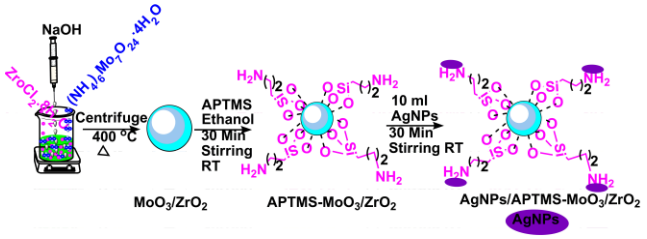

Fig1. Mechanism of AgNPs/APTMS-MoO_3/ZrO_2 nanocomposite

B. UV-Visible studies on AgNPs/APTMS-MoO_3/ZrO_2 nanocomposite

Figure 2 (A-C) shows, (A) MoO_3/ZrO_2, (B) TSC capped AgNPs and (C) AgNPs/APTMS-MoO_3/ZrO_2 nanocomposite. MoO_3/ZrO_2 was observed by the two excitation wave length 275 nm and 355 nm, that was charge transfer transition in O^{2-}-Zn^{4+} and tetragonal polymorph of ZrO_2 [42]. A broad peak at 657 nm was displayed because of large size and aggregated of MoO_3 particles dispersed in ZrO_2 due to surface Plasmon resonance (SPR) as shown in **Fig. 2(A).** Figure **2(B)** shows the pure TSC capped AgNPs which was recorded at 442 nm [43]. AgNPs/APTMS-MoO_3/ZrO_2 nanocomposite was showed as broad peak and slightly shifted at 455 nm [44, 45] that means AgNPs was strongly coated on APTMS-ZrO_2/MoO_3 as shown in **Fig.2(C).**

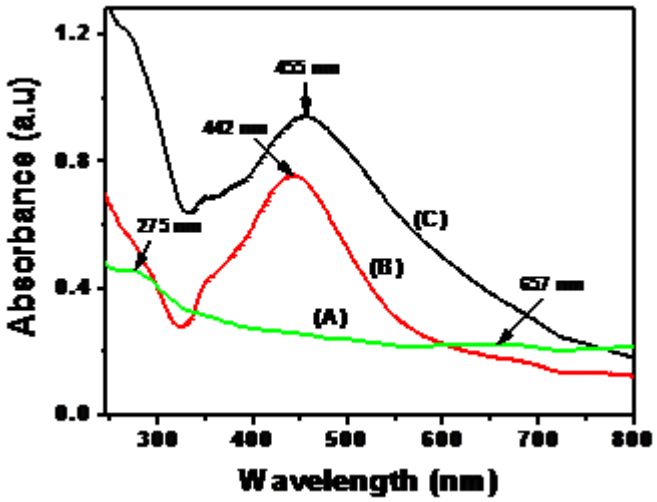

Fig. 2(A-C) UV-visible spectra of (A) MoO_3/ZrO_2, (B) AgNPs and (C) AgNPs/APTMS-MoO_3/ZrO_2 nanocomposite

C. FT-IR Characterization of AgNPs/APTMS-MoO_3/ZrO_2 nanocomposite

The FT-IR spectra of MoO_3/ZrO_2 and AgNPs/APTMS-MoO_3/ZrO_2 were displayed as shown in **Fig. 3(A&B).** MoO_3/ZrO_2 was recorded different stretching vibration band at 1014 cm^{-1}-1108 cm^{-1}, 800 cm^{-1}, 606 cm^{-1}, 3328 cm^{-1},

1622 cm^{-1}, 1358 cm^{-1} and 2325 cm^{-1} corresponding to Mo=O bond of terminal, Mo-O-Mo in the oxygen atom, Mo-O-Mo due to bending vibration mode [46], due to the stretching vibration of vibration O-H groups, the bending vibration of O-H, H…O-H bending vibration and for O-H stretching, respectively as shown in Fig.3A, in which ZrO_2 nanoparticles shows the broad and sharp peaks were delivered at 3328 cm^{-1} and 1622 cm^{-1} due to stretching and bending vibration of water. The peak was mentioned at 1358 cm^{-1} due to hydrogen peaks [47]. The band located at ~606 cm^{-1} corresponds to Zr–O vibration of tetragonal. The bond mentions that ZrO_2 powders are nanocrystals [48, 49] as shown in **Fig.3A**. The stretching vibration band at 2325 cm^{-1} was assigned to CO_2 with its peak intensity decreased due to calcinations at 400C. AgNPs/APTMS-MoO_3/ZrO_2 nanocomposite was completely exhibited the reduced peak intensity values and it confirmed the AgNPs strong interaction with APTMS-MoO_3/ZrO_2 nanocomposite as shown in **Fig.3B.**

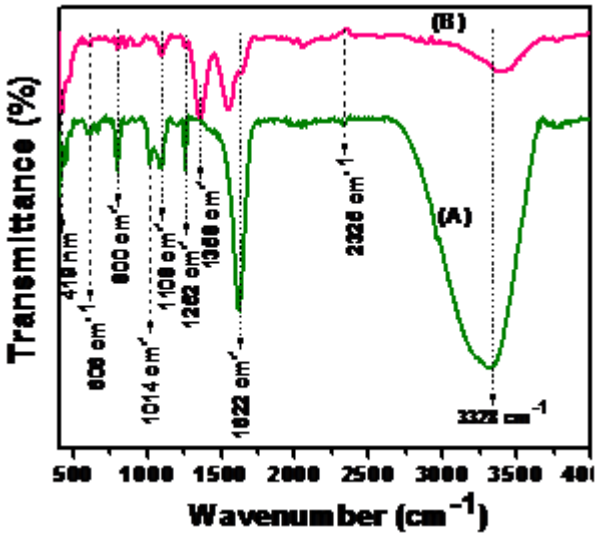

Fig. 3(A & B) FT-IR spectra of (A) MoO_3/ZrO_2, (B) AgNPs/APTMS-MoO_3/ZrO_2 nanocomposite

D. X-ray Diffraction of AgNPs/APTMS-MoO_3/ZrO_2 nanocomposite

The x-ray diffraction pattern of MoO_3/ZrO_2 and AgNPs/APTMS-MoO_3/ZrO_2 nanocomposite was displayed as shown in **Fig.4 (A&B).** MoO_3/ZrO_2 was showed the tetragonal and monoclinic phase at 400 ^oC, due to strong coated and strong interaction of MoO_3 on the ZrO_2 [50]. **Figure 4(A)** shows the calcinated ZrO_2/MoO_3, in which ZrO_2 has small intensity peaks at 2θ = 30.2 ^{o}, 34.5 ^{o}, 50.2 ^{o} and 60.2^o corresponding to the (101), (110), (200) and (211) with (JCPDS No.70-1769). It observes that tetragonal phase ZrO_2 [51]. Similarly, MoO_3 peaks were recorded at 10.9^o, 12.6^o, 25.3^o, 28.1^o, and 41.3^o. This confirmed the orthorhombic phase of MoO_3 and it was matched with the (JCPDS Card No.35-0609) as shown in **Fig. 4(A).** AgNPs/APTMs-MoO_3/ZrO_2 nanocomposite was exhibited with the developed the diffraction peak intensity as well as number diffraction peaks as shown in **Fig.4 (B).** This improvement is mainly due to AgNPs coated on APTMs-MoO_3/ZrO_2 with its diffraction peaks were indicated as red circle as shown in **Fig.4B.** The average crystallite sizes of the ZrO_2 nanocrystallites have been estimated by Scherer's formula:

$$D = K\lambda/\beta\cos\theta$$

where K = 0.9 is the shape factor, λ is the X-ray wavelength of Cu K_α radiation (0.1542 nm), θ is the Bragg angle and β is the full-width at half-maximum (FWHM) intensity peak (in units of radians). The average particles diameter of the AgNPs/APTMs MoO_3/ZrO_2 nanocomposite was calculated to be 5.12 nm for samples, respectively.

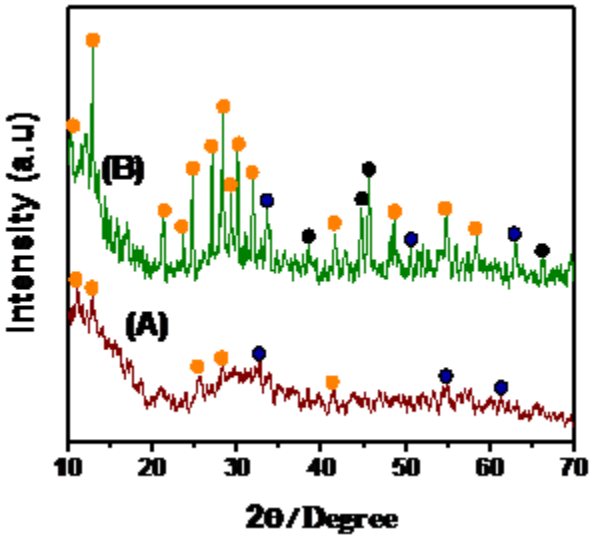

Fig. 4(A & B) X-ray Diffraction spectra of (A) MoO_3/ZrO_2 and (B) AgNPs/APTMS-MoO_3/ZrO_2 nanocomposite,

E. FESEM image of AgNPs/APTMS-MoO_3/ZrO_2 nanocomposite

AgNPs bound in calcined of APTMs-MoO_3/ZrO_2 nanocomposite and it is confirmed by SEM image as shown in **Fig.5 (A-C)**. The crowd of AgNPs impregnated in MoO_3/ZrO_2 image was recorded AgNPs was clearly displayed on APTMS-MoO_3/ZrO_2 nanocomposite at different place focused with same magnification of SEM image as shown in **Fig. 5(B).** According to SEM image of AgNPs were absolutely recorded about size 10 nm as shown in **Fig.5C.**

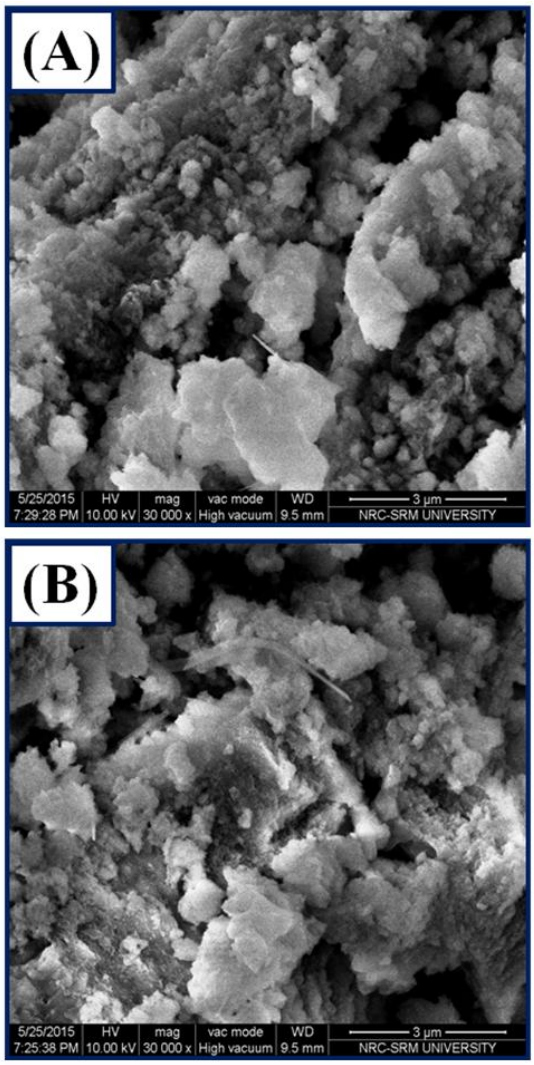

Fig. 5(A & B) SEM images of AgNPs/APTMS-MoO_3/ZrO_2 nanocomposite at magnification (A) 3 µM and (B) at different place 3 µM.

F. Photo catalytic Application of Methyl Parathion

Methyl parathion, which is mostly used as a pesticide in agriculture and excess amount of MP is being mixed with run off rain water and reached nearby water bodies, which causes ill effect to human beings and animals. This toxic effect is because of presence of NO_2 group and phosphate group. The conversion of NO_2 to NH_2 in methyl parathion by using AgNPs/APTMS-MoO_3/ZrO_2 nanocomposite catalyst under the visible light irradiation at different time 0 5 min, 10 min 15 min, 20 min, 25 min, 30 min, 35 min and 40 min (yellow to colorless) reduces toxic effect of MP to decreases with AgNPs/APTMS-MoO_3/ZrO_2 nanocomposite delivered as better reduction catalyst as well as acid catalyst in NO_2 to NH_2. This reaction was confirmed by UV-visible spectroscopy with its absorption peaks was recorded at 455 nm and 305 nm. Here, the peak at 455 nm was gradually decreased with 0 to 40 min as shown in **Fig.6A**. The rate constant of the reaction was calculated between plot of $\ln(C_t/C_0)$ and time as shown in **Fig.6B**. The first order kinetic was explained as follow:

$$\ln C_t/C_0 = -kKt = -k_{app}t \quad \ldots\ldots\ldots\ldots\ldots\ldots\ldots\ldots(1)$$

where

C_0 is the initial concentration of MP [mg L^{-1}],

C_t is the instant concentration of the sample at time t [mg L^{-1}],

The above equation clearly expressed the first order kinetic with rate constant of AgNPs/APTMS-MoO_3/ZrO_2 nanocomposite K = 9.0160 x 10^{-2} min^{-1} a shown **Fig. 5B**. The above said graph was confirmed that nanocatalyst of AgNPs interior in APTMS-MoO_3/ZrO_2 nanocomposite.

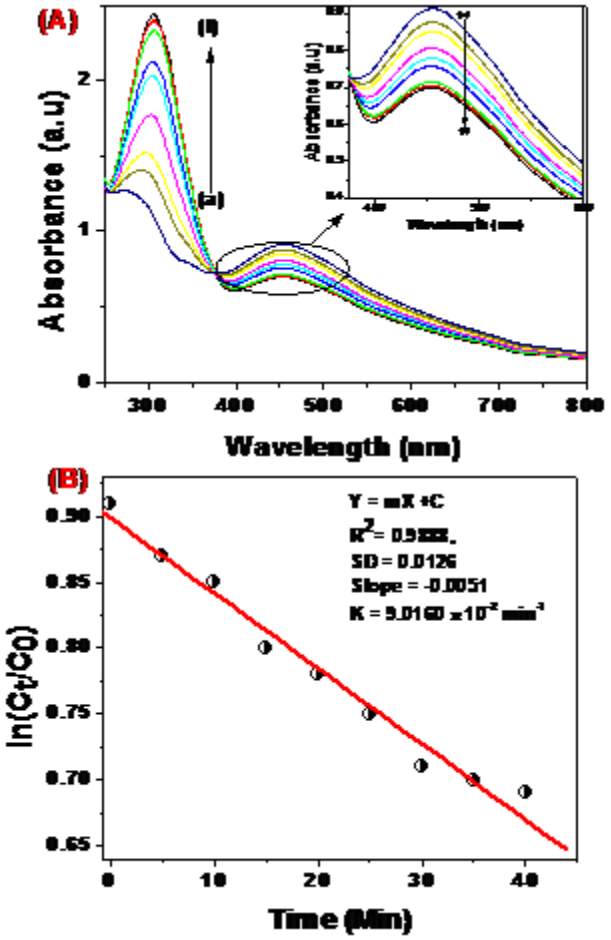

Fig. 6(A & B) UV-Vis spectra of Methyl parathion (A) and liquid with AgNPs/APTMS-MoO_3/ZrO_2 nanocomposites under visible light irradiation of (a-i) 0 min to 40 min. (B) Calibration plot.

G. Mechanism of catalytic degradation in presence of sunlight irradiation

The valence band holes (h^+VB) and conduction band electrons (e^-CB) was formed by visible light. The materials absorption of visible light photo of energy was greater than or equal to its band gap ($h\nu \geq$ EBG). The holes were easily oxidation of organic compounds to form hydroxyl radicals. The electrons were easily reduction and oxidation with generation Superoxide radicals [52]. The above said mechanism was applied in organophosphate degradation and

The AgNPs was existing SPR under the visible light region. It can motivate the trapped electrons to transfer and acceptors. AgNPs is not efficient photocatalyst in visible light irradiation to carry out the photocatalytic reaction. Synergetic effect mechanism was displayed in this photocalytic mechanism as shown in **Fig.7.** MoO_3/ZrO_2 is separated valence band (VB) and conduction band (CB) under visible light. The excited state of MoO_3/ZrO_2 electron was transfer to conduction band of AgNPs and increased the SPR effect of AgNPs. Visible light excitation and SPR effect was induced the photocatalytic degradation of MP on AgNPs/APTMS-MoO_3/ZrO_2 nanocomposite as shown in **Fig.7**

AgNPs/APTMS-MoO_3/ZrO_2 nanocomposite formed electrons and holes under visible light irriadtion. The h^+_{VB} was oxidized on H_2O to generated (·OH) and delivered the O^{2-} and H^+ [49]. MoO_3/ZrO_2 conduction band of e^- was trapped by AgNPs and form SPR effect of Ag^{e-}. This was used to oxidize on MP and get degradation products such as Methoxy paraoxon (MPO), 4-Nitrophenol (4-NP), Hydroquinone (HQ), 2-hydroxy hydroquinone (HHQ), Aliphatic acid (AA), Formic acid (FA) and CO_2 [53-55]. Here, the major activity of AgNPs above said process is electron holding, SPR effect development, recombination of electron–hole pairs and development of charge transfer efficiency as shown in **Fig.7.**

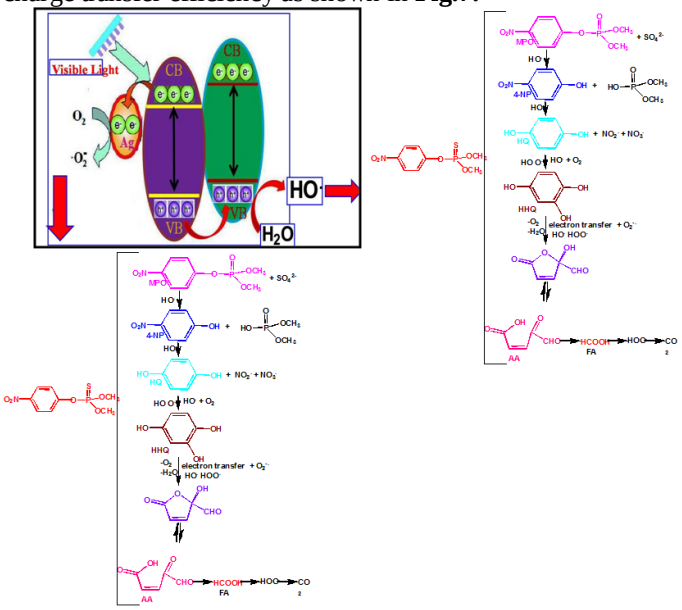

Fig.7 Degradation mechanism of MP in presence of AgNPs/APTMS-MoO_3/ZrO_2 under visible light.

IV. CONCLUSION

In this study, the AgNPs/APTMS-MoO_3/ZrO_2 and MoO_3/ZrO_2 was synthesized by using co-precipitation method by precursor of $ZrOCl_2 \cdot 8H_2O$ presence of ammonium heptamolybdate under basic medium pH 10 at room temperature. The synthesize MoO_3/ZrO_2 was completely undergo calcination at 120°C and the resulting AgNPs/APTMS-MoO_3/ZrO_2 was collected. And characterization was done with various experimental techniques to study its shape, size and its optical properties. From FT-IR studies it is confirmed that carboxylate ions are strongly coordinated with AgNPs/APTMS-MoO_3/ZrO_2 and MoO_3/ZrO_2. The catalytic decomposition of Methyl parathion was investigated using AgNPs/APTMS-MoO_3/ZrO_2 under Visible light irradiation. The decay of the MP follows the pseudo first order kinetics with a rate constant of 9.8 x 10^{-2} min^{-1}. The decomposition rate is superior compared to other photocatalytic decomposition method.

Acknowledgements

The authors acknowledge the Management, and Department of Chemistry, GKM College of Engineering & Technology, New Perungalathur, Chennai–600063, India. The authors also acknowledge SRM University provided FE-SEM and University of Madras, Chennai-25 for providing XRD.

References

[1] I.K. Konstantinou, A.K. Zarkadis, T.A. Albanis, "Photodegradation of Selected Herbicides in Various Natural Waters and Soils under Environmental Conditions" J. Environ. Qual. vol. 30, pp.121-130, February 2001.

[2] X. Zhu, C. Yuan, Y. Bao, J. Yang, Y. Wu, "Photocatalytic degradation of pesticide pyridaben on TiO_2 particles" J. Mol. Catal. A: Chem. vol. 229, pp. 95–105, December 2005.

[3] E. Moctezuma, E. Leyva, G. Palestino, H. de Lasa, "Photocatalytic degradation of methyl parathion: Reaction pathways and intermediate reaction products" J. Photochem. Photobiol. A: Chem. vol. 186, pp. 71-84, July 2007.

[4] L. Wei, C. Shifu, Z. Wei, Z. Sujuan, "Titanium dioxide mediated photocatalytic degradation of methamidophos in aqueous phase" J. Hazard. Mater.vol. 164, pp. 154–160, August 2009.

[5] T. Aungpradit, P. Sutthivaiyakit, D. Martens, S. Sutthivaiyakit, A.A..F Kettrup, "Photocatalytic degradation of triazophos in aqueous titanium dioxide suspension: Identification of intermediates and degradation pathways" J. Hazard. Mater.vol. 146, pp. 204–213, December 2007.

[6] B. Yu, J. Zeng, L. Gong, M. Zhang, L. Zhang, X. Chen, B. Yu, J. Zeng, L. Gong, M. Zhang, L. Zhang, X. Chen "Investigation of the photocatalytic degradation of organochlorine pesticides on a nano-TiO_2 coated film" Talanta vol. 72, pp. 1667–1674, March 2007.

[7] T. Bhaskar, K.R. Reddy, C.P. Kumar, M.R.V.S. Murthy, K.V.R. Chary, "Characterization and reactivity of molybdenum oxide catalysts supported on zirconia" Appl. Catal. A vol. 211, pp. 189–201, April 2001.

[8] H. Ranjan Sahu, G. Ranga Rao "Characterization of combustion synthesized zirconia powder by UV-Vis, IR and other techniques" Bull. Mater. Sci. vol. 23, pp. 349-354, October 2000.

[9] S. Shukla, S. Seal, "Mechanisms of Room Temperature Tetragonal Phase Stabilization in Zirconia" T. Int. Mater. Rev. vol. 50(1), pp. 45-64, 2005.

[10] J. Liang, X. Jiang, G. Liu, Z. Deng, J. Zhuang, F. Li, Y. Li, "Characterization and synthesis of pure ZrO_2 nanopowders via sonochemical method", Mater. Res. Bull., Vol.38, pp.161-168, January 2003.

[11] Mao, D., Lu, G., Chen, Q. "Influence of calcination temperature and preparation method of TiO_2–ZrO_2 on conversion of cyclohexanone oxime to ε-caprolactam over B_2O_3/TiO_2–ZrO_2 catalyst". Appl. Catal. A vol. 263, pp. 83-89, May 2004.

[12] N. Chandra, D.K. Singh, M. Sharma, R.K. Upadhyay, S.S. Amritphale, S.K. Sanghi, "Synthesis and Characterization of Nano-Sized Zirconia Powder Synthesized by Single Emulsion-Assisted Direct Precipitation" J. Colloid Interface Sci., vol. 342, pp. 327-332, October 2009.

[13] B. Zhu, C.R. Xia, X.G. Luo, " Transparent Two-Phase Composite Oxide Thin Films with High Conductivity, Thin Solid Films" vol. 385, pp. 209-214, April 2001.

[14] N.G. Petrik, D.P. Taylor, T.M. Orlando, "Laser-Stimulated Luminescence of Yttria-Stabilized Cubic Zirconia Crystals" J. Appl. Phys., vol. 85, pp. 6770-6776, May 1999.

[15] A. Bastianini, G.A. Battiston, R. Gerbasi, M. Porchia, S. Daolio, "Chemical Vapor Deposition of ZrO_2 Thin Films Using $Zr(NEt_2)_4$ as Precursor" J. Phys. IV France 05, vol. 4(5), pp. C5-525-C5-531, Jun1995.

[16] S.K. Maity, M.S. Rana, B.N. Srinivas, S.K. Bej, G.M. Dhar, T.S.R. Prasada, Characterization and evaluation of ZrO supported hydrotreating catalysts title J. Mol. Catal. A vol.153, pp. 121–127, August 2000.

[17] A. Calafat, L. Avil´an, J. Aldana, Appl. Catal. A, The influence of preparation conditions on the surface area and phase formation of MoO_3/ZrO_2 catalysts vol. 201, pp. 215–223, July 2000.

[18] A. Corma, "Inorganic Solid Acids and Their Use in Acid-Catalyzed Hydrocarbon Reactions" Chem. Rev., vol. 95, pp. **559-614**, February 1995.

[19] E. M. McCarron III, "β-MoO_3: a metastable analogue of WO_3. Chem. Soc., Chem. Commun. pp. 336-338, 1986.

[20] N. Sotani, "Studies on the Hexagonal Hydrate of Molybdenum Trioxide. The Physical Properties of the Hydrate and Its Changes on Heat Treatments in Air, in Hydrogen, and in a Hydrogen–thiophene Mixture" Bull. Chem. Sot. Jpn. vol. 48, No. 6, pp. 1820-1825, June 1975.

[21] W. Dong and B. Dunn, "Sol–gel synthesis and characterization of molybdenum oxide gels" Journal of Non-Crystalline Solids" vol. 225, pp. 135-140, April 1998.

[22] X.L. Li, J.F. Liu, Y.D. Li, "Low-temperature synthesis of large-scale single-crystal molybdenum trioxide .MoO3. nanobelts" Appl. Phys. Lett., vol. 81, pp. 4832-4834, December 2002.

[23] G.R. Patzke, A. Michailovski, F. Krumeich, R.d Nesper, J. D. Grunwaldt, A. Baiker, "One-Step Synthesis of Submicrometer Fibers of MoO_3" Chem. Mater. vol. 16, pp. 1126-1134, August 2004.

[24] A. Lagashetty, V. Havanoor, S Basavaraja, A .Venkataraman, "Synthesis of MoO3 and its polyvinyl alcohol nanostructured film" Bull. Mater. Sci., vol. 28, pp. 477-481, August 2005.

[25] L. Cai, P.M. Rao, X.L. Zheng, "Morphology-Controlled Flame Synthesis of Single, Branched, and Flower-like r-MoO_3 Nanobelt Arraystitle" Nano. Lett. vol.11, pp. 872–877, January 2011.

[26] H.C. Zeng, Chemical Etching of Molybdenum Trioxide: A New Tailor-Made Synthesis of MoO_3 Catalysts Inorg. Chem. vol. 37, pp. 1967-1973, October 1998.

[27] C. Julien, A. Khelfa, O.M. Hussain, G.A. Nazri, "Synthesis and characterization of flash-evaporated MoO_3 thin films" Journal of Crystal Growth" vol. 156, pp. 235-244, May 1995.

[28] J. Zhou, S.Z. Deng, N.S. Xu, J. Chen, J.C. She, "Synthesis and field-emission properties of aligned MoO_3 nanowires" Appl. Phys. Lett. vol. 83, pp. 2653-2655, 29 September 2003.

[29] S. Hu, X. Wang, "Single-Walled MoO3 Nanotubes" J. Am. Chem. Soc., vol. 130, pp. 8126-8127, February 2008.

[30] T. Xia, Q. Li, X.D. Liu, J. Meng, X. Q. Cao, "Morphology-Controllable Synthesis and Characterization of Single-Crystal Molybdenum Trioxide" J. Phys. Chem. B, vol. 110, pp. 2006-2012, January 2006.

[31] X.F. Yang, H. Tang, R.X. Zhang, H.J. Song, K.S. Cao," NaCl-assisted hydrothermal synthesis of high-quality crystalline α-MoO_3 nanobelts" Cryst. Res. Technol. Vol.46, No. 4, 409 – 412, 2011.

[32] J. S. Chen, Y.L. Cheah, S. Madhavi, X. W. Lou, "Fast Synthesis of r-MoO_3 Nanorods with Controlled Aspect Ratios and Their Enhanced Lithium Storage Capabilities" J. Phys. Chem. C, vol. 114, pp. 8675–8678, 2010.

[33] F. Leroux, L.F. Nazar, "Uptake of lithium by layered molybdenum oxide and its tin exchanged derivatives: high volumetric capacity materials" Solid State Ionics, vol. 133, pp. 37-50, August 2000.

[34] I. Shakir, M. Shahid, H.W. Yang, D.J. Kang, "Structural and electrochemical characterization of α-MoO_3 nanorod-based electrochemical energy storage devices" Electrochimica Acta, vol. 56, pp. 376-380, December 2010.

[35] C.V.S. Teddy, E.H. Walker Jr., C. Wen, S. Mho, "Hydrothermal synthesis of MoO_3 nanobelts utilizing poly(ethylene glycol)" Journal of Power Sources, vol. 183, pp. 330-333, 2008.

[36] L.Q. Mai, F. Yang, Y.L. Zhao, X. Xu, L. Xu, B. Hu, Y. Z. Luo, H. Y. Liu, Molybdenum oxide nanowires: synthesis & properties Materials Today, vol. 14, pp. 346-352, August 2011.

[37] S.H. Lee, Y.H. Kim, R. Deshpande, P.A. Parilla, E. Whitney, D.T. Gillaspie, K.M. Jones, A.H. Mahan, S.B. Zhang, A.C. Dillon, "Reversible Lithium-Ion Insertion in Molybdenum Oxide Nanoparticles" Adv. Mater., vol. 20, pp. 3627–3632, September 2008.

[38] L. Campanella, G. Pistoia, "MoO_3: A New Electrode Material for Nonaqueous Secondary Battery Applications" J. Electrochem. Soc. vol. 118 (12), pp. 1905-1908, may 1971.

[39] N. Margalit, "Discharge Behavior of Li / MoO_3 Cells" Journal of the Electrochemical Society, vol. 121, pp. 1460-1461, June 1974.

[40] F .Wang, W. Ueda, "High catalytic efficiency of molybdenum trioxide in the benzylation of arenes and as investigation of reaction mechanism" Chem. Eur. Journals, vol. 15, pp. 742-754, November 2008.

[41] P. Pichat, M. Mozzanega, C. Hong-Van, "Room temperature photo assisted formation of hydrogen molybdenum bronzes with alcohol as hydrogen source" J Phys Chem. vol. 92, pp. 464-467. July 1988.

[42] B.R. Faughanan, R.S. Crandall, "Optical properties of mixed oxide WO_3 and MoO_3 electrochromic film" Appl. Phys Latter, vol.31, pp. 834-835, 1977.

[43] G. Herrera, N. Montoya, A. Dome´nech-Carbo, J. Alarco´n, "Synthesis, characterization and electrochemical properties of iron-zirconia solid solution nanoparticles prepared using a sol–gel technique" : Phys. Chem. Chem. Phys. vol.15, pp. 19312-19320. September 2013.

[44] P. R. Kumar, S. Vivekanandhan, M. Misra, A. Mohanty, N. Satyanarayana, "Soybean (Glycine max) Leaf Extract Based Green Synthesis of Palladium Nanoparticles" J. Biomater. Nanobiotechnol. Vol. 3, pp. 14-19, December 2012.

[45] T. Fujita, K. Ijima, N. Mitsui, K. Mochiduki, Y. Saito, "Coloration Related to Nanostructure of Yttria-Stabilized Cubic Zirconia Single Crystal Implanted with Ag Ions" Jpn. J. Appl. Phys., vol. 46, pp. 7362, November 2007.

[46] F. Gonella, G. Mattei, P. Mazzoldi, G. Battaglin, A. QuarantaG," Structural and Optical Properties of Silver-Doped Zirconia and Mixed Zirconia−Silica Matrices Obtained by Sol−Gel Processing" Chem. Mater. vol. 11, pp. 814-821. Fruary 1999.

[47] Nyquist, R.A., Putzig, C.L., Leugers M.A. eds. (1997) Handbook of Infrared and Raman spectra of Inorganic Compounds and Organic Salts. 295-350. Academic Press, New York.

[48] Y.F. Gao, Y. Masuda, H. Ohta and K. Koumoto, "Room-Temperature Preparation of ZrO_2 Precursor Thin Film in an Aqueous Peroxozirconium-Complex Solution" Chemist. Mater. vol.16, pp. 2615–2622, June 2004.

[49] C. Pecharroman, M. Ocana and C.J. Serna, "Optical constants of tetragonal and cubic zirconias in the infrared" J. Applied Phys., vol. 80, pp. 3479–3483, June 1996.

[50] J.R. Sohn, S.G. Cho, Y.I. Pae, S. Hayashi, Characterization of Vanadium Oxide–Zirconia Catalyst J. Catal.vol. 159, pp. 170-177, March 1996.

[51] X. Xu, X. Wang, "Fine tuning of the sizes and phases of ZrO_2 nanocrystals," Nano Research, vol. 2, No. 11, pp. 891–902, October 2009.

[52] J.C. Wu, Photocatalytic reduction of greenhouse gas CO_2 to fuel. Catal. Surv. Asia. vol. 13, pp. 30–40, February 2009.

[53] M. Anpo, H. Yamashita, Y. Ichihashi, S. Ehara, "Photocatalytic reduction of CO_2 with H_2O on various titanium oxide catalysts" J Electroanal Chem vol. 396, pp. 21–26, 1995.

[54] S.S. Tan, L. Zou, E. Hu. E, "Photocatalytic reduction of carbon dioxide into gaseous hydrocarbon using TiO_2 pellets" Catal. Today vo. 115, pp 269–273, June 2006.

[55] Q.H. Zhang, WD. Han, Y.J. Hong, J.G. Yu, "Photocatalytic reduction of CO_2 with H_2O on Pt-loaded TiO_2 catalyst. Catal Today vol. 148, pp. 335–340, November 2009.